Temporal Shelter Hypothesis: Planck-Calibrated Operational Frames and Observer-Relative Readout

A Conservative Programmatic Framework with a Base-Invariant Ladder Estimate

Independent Research Collaboration on Black Hole and Cosmology Concepts (IRCBHC)

Project identity for an independent research program on black-hole and cosmological time concepts

June 3, 2026

Abstract

This paper reformulates the Temporal Shelter Hypothesis as an observer-relative operational framework rather than a claim about literal habitation inside ordinary astrophysical black holes. The central claim is narrow: long biological and civilizational histories require locally coherent proper-time accumulation, while the external reconstruction of that history may depend on the operational mismatch between observer frames.

The revised framework distinguishes three levels. First, the Planck scale is treated as an operational baseline for limiting units and readout resolution, not as a material ether or preferred inertial rest frame. Second, the present observer frame is calibrated using the electron Compton wavelength as a physical step-length anchor, yielding an operational frame index

$$r_{\text{phys}} = \log_2\left(\frac{\lambda_C}{l_P}\right) = \log_2\left(\frac{\lambda_C/c}{t_P}\right) \approx 76.99.$$

Third, gravitational or phase-density environments modify effective readout factors between frames.

The paper introduces a phase-capacity Race Protocol in which a normalized progress share k and an internal recurrence share R satisfy $k^2 + R^2 = 1$. Applying this protocol to the Compton/Planck frame ratio gives

$$k = \frac{\log_b X}{\log_b(2X)}, \qquad X = \frac{\lambda_C}{l_P},$$

which is invariant under changes of logarithmic base because the physical boundary condition is the doubling of the scale ratio X, not the coordinate base used to describe it. Numerically this yields

$$k = \frac{76.99}{77.99}, \qquad R \simeq 0.1596, \qquad \Gamma_{\text{ladder}} = 1/R \simeq 6.26.$$

This factor is classified as a heuristic compression-depth estimator, not as a direct empirical measurement of cosmological time dilation.

The framework also identifies candidate quantitative test domains: environmental dependencies of Type Ia supernova light curves, reported but debated log-periodic redshift structure, and log-periodic constraints from CMB and gravitational-wave searches in discrete-scale-invariant models. A mock-data sensitivity test is included for the structurally predicted frequency $f_{mstruct} = 1/\log_{10} 2$. None of these is presented as established evidence. The intended test is a composite pattern of weak, structured, observer-relative residuals that cannot be reduced to a single anomaly. The manuscript is therefore a constrained research program rather than a completed cosmological model.

Keywords: proper time; Planck scale; electron Compton wavelength; operational frames; gravitational time dilation; horizons; observer-dependent readout; lapse function; biological time; cosmology; CMB residuals.

1. Introduction

Life requires time. More precisely, life requires locally usable time: stable cycles, memory, chemistry, replication, repair, selection, and long-term environmental continuity. A technological civilization requires not merely years in a coordinate sense, but an enormous accumulation of ordered local events.

The standard answer is straightforward: the universe is old enough. In the standard cosmological model, the universe has a finite but very large cosmic history, inferred from the expansion history, cosmic microwave background (CMB), baryon acoustic oscillations, nucleosynthesis, and large-scale structure [10, 7, 8]. This explanation is empirically powerful and is not rejected here.

However, relativity teaches that time is not a single universal background parameter. Proper time is local and path-dependent. Clocks in different gravitational conditions, or along different worldlines, do not necessarily accumulate the same elapsed time [2, 4, 5]. This motivates a narrower question: could long biological time be partly understood as a local proper-time condition produced by temporal protection within a large gravitational or horizon-adjacent readout domain?

This paper calls that possibility the *Temporal Shelter Hypothesis*:

> A region embedded in a sufficiently large, smooth, co-falling gravitational or phase-density domain may experience long, stable internal time while appearing slowed, compressed, black-hole-like, or poorly readable relative to a sufficiently different external observer.

The aim is not to replace standard cosmology with an alternative model. The aim is to formulate a constrained hypothesis whose consistency conditions, failure modes, and possible observational footprints can be stated explicitly.

2. What the Hypothesis Does Not Claim

To avoid misunderstanding, the Temporal Shelter Hypothesis does not claim:

1. that Earth is proven to be inside a black hole in any absolute or ordinary astrophysical sense;
2. that ordinary stellar black holes are habitable;
3. that time dilation alone is sufficient for life;
4. that standard cosmology is refuted;
5. that horizons are automatically creative environments;
6. that gravitational shelter removes the need for chemistry, energy gradients, and matter.

The claim is narrower:

> Strong relative time dilation may be one possible physical mechanism for producing long internal histories within externally constrained readout domains.

The question is therefore not "Are we inside a black hole?" in an absolute ontological sense. The safer question is: can a horizon-adjacent or strongly time-dilated domain provide one of the local temporal conditions required for biological complexity?

3. Planck-Calibrated Operational Frame Structure

The present formulation treats observable physical differences as arising from transformations between operational frames rather than from absolute hidden locations. The word "frame" is used operationally: it denotes the scale, clocking, and readout convention by which an observer reconstructs physical quantities.

The Planck scale is treated here as an operational baseline rather than merely as a small length. In this interpretation, the Planck frame is the limiting reference layer before gravitational readout distortion is introduced. It is not a material frame, not an ether, and not a preferred inertial rest frame in the classical sense. It is a baseline of operational resolution.

3.1. Calibration of the Present Operational Frame

The present physical frame can be calibrated without appealing to an inaccessible external observer. Use the unreduced electron Compton wavelength as the step-length anchor:

$$\lambda_C = \frac{h}{m_e c}. \tag{1}$$

Numerically,

$$\lambda_C \simeq 2.42631023867 \times 10^{-12} \text{ m}. \tag{2}$$

Define one operational tick as the time required for the propagation pattern to traverse one such step-length at invariant propagation speed c:

$$T_{\text{tick}} = \frac{\lambda_C}{c}. \tag{3}$$

This gives

$$T_{\text{tick}} \simeq 8.0933 \times 10^{-21} \text{ s}. \tag{4}$$

Using the Planck floor

$$l_P \simeq 1.616 \times 10^{-35} \text{ m}, \qquad t_P \simeq 5.391247 \times 10^{-44} \text{ s}, \tag{5}$$

the frame index of the present operational scale is

$$r_{\text{phys}} = \log_2 \left(\frac{T_{\text{tick}}}{t_P} \right) = \log_2 \left(\frac{\lambda_C}{l_P} \right) \simeq 76.99. \tag{6}$$

This number is not introduced as a mystical integer layer. The ladder is continuous; integer frames are only markers. The value $r_{\text{phys}} \approx 76.99$ is an operational calibration of the present frame against the Planck floor using a laboratory-defined particle scale.

3.2. Readout Factors and Logarithmic Rank

Let two observer frames be denoted by

$$A, \qquad B. \tag{7}$$

Let each frame possess an effective readout factor

$$\alpha_A, \qquad \alpha_B. \tag{8}$$

In ordinary relativistic examples, α may be identified with a lapse-like factor. In a Schwarzschild exterior, for example,

$$\alpha(r) = \sqrt{1 - \frac{2GM}{rc^2}}. \tag{9}$$

More generally, α denotes the factor by which internal cycle accumulation is reconstructed by another frame.

A logarithmic operational rank may then be defined by

$$r = -\log_b(\alpha), \tag{10}$$

where $b > 1$ is a chosen scaling base. The binary choice $b = 2$ is useful when one wishes to express frame differences in bit-like or doubling units, but the base is not the physical source of the effect. The physical content is the ratio of readout factors.

For two frames,

$$\Delta r = r_B - r_A. \tag{11}$$

Using the definition above,

$$b^{\Delta r} = \frac{\alpha_A}{\alpha_B}. \tag{12}$$

Thus the earlier schematic expression

$$\Pi_{A\to B} \sim 2^{\Delta r} \tag{13}$$

should not be read as an unsupported new force law. It is a logarithmic representation of the readout ratio when the base is chosen to be 2:

$$2^{\Delta r} = \frac{\alpha_A}{\alpha_B}. \tag{14}$$

3.3. Minimal Action of the Readout Transform

Observable reconstruction between frames is represented schematically by

$$\Pi_{A\to B}. \tag{15}$$

For time-like quantities, the minimal readout rule is

$$T_B = \Pi^{(T)}_{A\to B}(T_A) = \frac{\alpha_A}{\alpha_B} T_A. \tag{16}$$

For frequencies or rates,

$$\nu_B = \Pi^{(\nu)}_{A\to B}(\nu_A) = \frac{\alpha_A}{\alpha_B} \nu_A, \tag{17}$$

which is the usual gravitational-redshift scaling when α is identified with a relativistic lapse.

For inferred mass, the paper uses only the operational proportionality

$$m_B(A) \propto \frac{\Pi_{A\to B}(N_{\text{cycles}})}{T_B}, \tag{18}$$

without claiming a completed mass theory. This is meant only to show how an observer-dependent mass readout could be formulated, not to replace the standard local rest mass definition.

The central proposal is that many quantities usually treated as absolute may instead be frame-read quantities:

$$T, \quad m, \quad L, \quad \mathcal{R}_{\text{horizon}}. \tag{19}$$

By contrast, accumulated internal cycle count is treated as operationally invariant:

$$N_{\text{cycles}} = \text{invariant}. \tag{20}$$

The fundamental distinction is therefore:

$$\text{invariant internal accumulation} \neq \text{observer-invariant readout}. \tag{21}$$

3.4. Why the Scaling Base Does Not Drive the Physics

The choice of base does not create the physical effect. A useful analogy is a family of concentric arcs. If arc length is written as

$$A_n = \theta r_n, \tag{22}$$

and the radii differ by terms proportional to a fixed geometric coefficient such as π, then differences between arcs may contain π as a single coefficient:

$$A_m - A_n = \theta\pi \sum_{j=n+1}^{m} k_j. \tag{23}$$

Even if the k_j grow rapidly, π itself does not compound into $\pi^2, \pi^3, \ldots$. The growth belongs to the sequence, not to the fixed geometric coefficient.

The same caution applies here. The base b, including the binary choice $b = 2$, is a coordinate convention for expressing rank differences. The physical growth or suppression is carried by the readout factor α and by the physical conditions that determine it, not by the base itself.

A temporal shelter is therefore not defined primarily as a location inside a deep gravitational well. It is defined as a domain in which local proper-time accumulation remains coherent while external reconstruction differs systematically across operational frames.

4. Phase-Capacity Race Protocol and the Origin of the Frame Ratio

The preceding frame-ladder notation gives an operational index $r_{\text{phys}} \simeq 76.99$ for the present electron-Compton frame relative to the Planck floor. This section adds the missing dynamical link between that frame index and the time-slowdown calculation. The aim is not to introduce a second independent postulate, but to express the same idea in the language of finite phase capacity.

4.1. Two-Channel Capacity Law

Let a closed operational system possess a normalized per-cycle phase capacity. This capacity may be divided between two mutually limiting channels:

$$k = \text{external progress or frame-advance share,} \tag{24}$$

$$R = \text{internal recurrence or clock-return share.} \tag{25}$$

The minimal closed budget is taken to be quadratic:

$$k^2 + R^2 = 1. \tag{26}$$

This is the same mathematical form as the ordinary Lorentz factor, but here it is read operationally: a system cannot spend the same normalized phase capacity twice. The more capacity assigned to external progress, the less remains available for internal recurrence.

Since a clock measures internal recurrence, the internal tick-rate relative to the reference recurrence is

$$R(k) = \sqrt{1 - k^2}. \tag{27}$$

The corresponding external slowdown factor is therefore

$$\Gamma_{\text{phase}}(k) = \frac{1}{R(k)} = \frac{1}{\sqrt{1 - k^2}}. \tag{28}$$

This equation is not an additional assumption after special relativity. It is the operational reading of the same invariant tradeoff: internal cycles are counted more slowly by an external reference when the progress share approaches unity.

4.2. Wave-Mean Justification of the Quadratic Form

The square in Eq. (26) can be motivated without assuming a primitive spacetime metric. Suppose a cyclic internal process is maintained by two opposed wave interactions. Let the normalized progress share be

$$k = \frac{v}{c}. \tag{29}$$

The forward and backward interaction frequencies are then schematically

$$f_+ = f_0(1 + k), \qquad f_- = f_0(1 - k). \tag{30}$$

A closed recurrence requires a round-trip phase matching, so the effective internal rate is the geometric mean rather than the arithmetic mean:

$$f_{\text{int}} = \sqrt{f_+ f_-} = f_0\sqrt{(1 + k)(1 - k)} = f_0\sqrt{1 - k^2}. \tag{31}$$

Thus the normalized internal recurrence factor is

$$R = \frac{f_{\text{int}}}{f_0} = \sqrt{1 - k^2}, \tag{32}$$

which gives Eq. (26). In this reading, the Lorentz-like factor is the macroscopic expression of a bidirectional phase-return condition.

4.3. Extraction of a Frame-Ladder Progress Share

The frame index obtained earlier is

$$r_{\text{phys}} = \log_2\left(\frac{\lambda_C}{l_P}\right) \simeq 76.99. \tag{33}$$

A minimal way to convert this frame rank into a progress share is to compare the active frame depth with the next closure level:

$$k_{\text{ladder}} = \frac{r_{\text{phys}}}{r_{\text{phys}} + 1}. \tag{34}$$

This construction has a clear operational meaning. The numerator represents the already accumulated frame depth of the present operational scale relative to the Planck floor. The denominator represents the same depth plus one additional closure step. The ratio therefore measures how close the current frame is to the next closure limit when expressed as a normalized progress share.

With

$$r_{\text{phys}} = 76.99, \tag{35}$$

one obtains

$$k_{\text{ladder}} = \frac{76.99}{77.99} = 0.9871778433\ldots. \tag{36}$$

Substitution into Eq. (27) gives

$$R_{\text{ladder}} = \sqrt{1 - \left(\frac{76.99}{77.99}\right)^2} = 0.1596241947\ldots. \tag{37}$$

Therefore

$$\Gamma_{\text{ladder}} = \frac{1}{R_{\text{ladder}}} = \frac{1}{\sqrt{1 - \left(\frac{76.99}{77.99}\right)^2}} = 6.26471173\ldots. \tag{38}$$

The interpretation is straightforward: if the ratio 76.99/77.99 is accepted as the ladder-derived progress share, then the associated internal recurrence is read at about 15.96% of the reference recurrence rate, or equivalently as about 6.26 times slower by the reference observer.

4.4. General Rank Formula and Base-Invariant Boundary

For a general frame rank $r > 0$, the binary ladder expression may be written as

$$k(r) = \frac{r}{r + 1}. \tag{39}$$

Then

$$R(r) = \sqrt{1 - \left(\frac{r}{r+1}\right)^2} = \frac{\sqrt{2r+1}}{r+1}, \tag{40}$$

and

$$\Gamma(r) = \frac{r+1}{\sqrt{2r+1}}. \tag{41}$$

For $r = 76.99$, Eq. (41) reproduces Eq. (38).

A possible ambiguity arises if the same physical ratio is expressed in another logarithmic base. Let

$$X = \frac{\lambda_C}{l_P}. \tag{42}$$

In base b, the rank is

$$r_b = \log_b X. \tag{43}$$

However, the next physical closure boundary is not bX. The physical boundary used in the binary structural ladder is the doubling of the scale ratio:

$$X \longrightarrow 2X. \tag{44}$$

Therefore the correct base-independent progress share is

$$k_b = \frac{\log_b X}{\log_b(2X)}. \tag{45}$$

Because logarithmic ratios are base-invariant,

$$\frac{\log_b X}{\log_b(2X)} = \frac{\ln X}{\ln(2X)} = \frac{\log_2 X}{\log_2(2X)}. \tag{46}$$

Thus the numerical progress share does not depend on the coordinate base used to describe the ladder:

$$k_b = \frac{76.99}{77.99} \simeq 0.98718. \tag{47}$$

This resolves a potential objection. The slowdown estimate does not change merely because one rewrites the ladder in a finer or coarser logarithmic base. What matters is the physical boundary condition $X \to 2X$, not the chosen logarithmic coordinate.

This compact formula separates three claims:

1. the kinematic-capacity claim, $k^2 + R^2 = 1$, which produces the slowdown factor;
2. the frame-ladder claim, $X = \lambda_C/l_P$, which assigns a physical operational ratio;
3. the boundary claim, $X \to 2X$, which defines the next closure level.

The first claim is the robust Race-Protocol core. The second and third claims are model choices that must be justified by the chosen frame architecture.

4.5. Status of the Numerical Result

The number $6.26471173\ldots$ should therefore be classified carefully. It is not a free numerical fit. Once r_{phys} and the rule $k = r/(r+1)$ are accepted, it follows algebraically. However, it should not yet be advertised as an empirical prediction of a completed cosmological model. Its correct status in the present manuscript is:

> A frame-ladder consequence of applying the Race Protocol to the electron-Compton-to-Planck operational rank.

This classification is important. It makes the calculation useful while avoiding the stronger claim that the universe, a galaxy, or a biological domain has already been shown to possess this exact shelter factor.

Quantity	**Value**	**Interpretation**
r_{phys}	76.99	Electron-Compton operational rank above the Planck floor
k_{ladder}	$76.99/77.99 = 0.9871778433\ldots$	Normalized progress share toward the next closure level
R_{ladder}	$0.1596241947\ldots$	Remaining internal recurrence share
Γ_{ladder}	$6.26471173\ldots$	External readout slowdown factor

4.6. Connection to Temporal Shelter

The temporal-shelter factor introduced later in this paper was written as

$$\mathcal{S} = \frac{T_{\text{bio}}}{T_{\text{ext}}}. \tag{48}$$

The Race-Protocol calculation supplies one possible operational mechanism for such a factor:

$$\mathcal{S}_{\text{ladder}} \sim \Gamma_{\text{ladder}}. \tag{49}$$

In the minimal electron-Compton ladder example,

$$\mathcal{S}_{\text{ladder}} \sim 6.26. \tag{50}$$

This is a moderate shelter factor, not an extreme horizon factor. It is therefore best interpreted as a demonstration that the framework can generate definite observer-relative time-readout factors from structural ratios. Much stronger shelter factors would require either k much closer to unity or an independent lapse/readout factor $\alpha \ll 1$.

5. Empirical Cross-Calibration with Reported Redshift Periodicity (Exploratory)

The binary ladder above uses $b = 2$ as a structurally minimal coordinate choice. This section explores whether a reported independent cosmological log-periodic scale, if confirmed, would alter the ladder slowdown estimate. The purpose is not to claim that the scale is real, but to test the internal consistency of the framework under a different descriptive base.

5.1. The Karlsson Periodicity as a Controversial Observational Claim

Periodic clustering in quasar and galaxy redshifts has been reported since the 1970s. The most discussed signal is the Karlsson period [27, 28], with a logarithmic spacing

$$\Delta \log_{10}(1 + z) \approx 0.089. \tag{51}$$

A recent re-analysis by Mal et al. [29] reports a Karlsson-type periodicity in survey data at approximately the 95% confidence level. This result remains debated and may be attributable to selection effects, survey-window artifacts, aliasing, or statistical fluctuations. It is therefore not treated here as an established fact.

5.2. Cross-Calibration Check

If, purely for exploratory purposes, the reported spacing is interpreted as a log-period of a discrete scale structure, the corresponding scaling ratio is

$$b_{\mathrm{K}} = 10^{0.089} \approx 1.227. \tag{52}$$

This value is not used to replace the binary structural base. It is used only to check whether the Race-Protocol slowdown estimate is sensitive to a change of logarithmic coordinate.

The operational frame rank in this alternative coordinate is

$$r_{\mathrm{K}} = \log_{b_{\mathrm{K}}} \left(\frac{\lambda_C}{l_P} \right) = \frac{\log_2(\lambda_C / l_P)}{\log_2(b_{\mathrm{K}})}. \tag{53}$$

Although r_{K} is numerically different from r_2, the correct progress share is not $r_{\mathrm{K}}/(r_{\mathrm{K}} + 1)$. The next physical boundary remains $X \to 2X$. Therefore

$$k_{\mathrm{K}} = \frac{\log_{b_{\mathrm{K}}} X}{\log_{b_{\mathrm{K}}}(2X)} = \frac{\log_2 X}{\log_2(2X)} = \frac{76.99}{77.99}. \tag{54}$$

Consequently,

$$\Gamma_{\mathrm{ladder}} \simeq 6.26 \tag{55}$$

is invariant under this change of logarithmic coordinate.

If the reported Karlsson-type spacing is physically real, it would more naturally correspond to a sub-rung, harmonic, or observational projection of the ladder rather than a replacement of the doubling boundary. Its relationship to the operational ladder is therefore a future test question, not a premise of the present framework.

5.3. Status of This Section

This section is exploratory. The core ladder estimate does not depend on the reality of redshift periodicity. If future surveys definitively rule out Karlsson-type periodicity, the empirical cross-calibration branch is weakened or removed, but the binary operational calibration and observer-relative readout framework remain unaffected.

6. The Biological Time Problem

A biological civilization requires at least five conditions:

1. stable matter;
2. persistent energy gradients;
3. low destructive flux;
4. chemical memory;
5. long-duration local time.

The fifth condition is often assumed rather than isolated. But if local elapsed time is observer-dependent, then the existence of billions of biological years may itself be treated as a physical condition requiring explanation.

Let T_{bio} be the minimum internal time required for biological evolution, and let T_{ext} be the interval assigned to the same domain by a chosen external readout convention. Define the shelter factor

$$\mathcal{S} = \frac{T_{\text{bio}}}{T_{\text{ext}}}. \tag{56}$$

A temporal shelter exists when

$$\mathcal{S} \gg 1. \tag{57}$$

This does not mean that internal observers feel slowed. It means that the internal domain can support a long developmental history while an external frame reads the same domain as slowed, compressed, or incomplete.

7. Gravitational Time Dilation as a Concrete Readout Example

In a static Schwarzschild-like exterior approximation, a stationary clock at radius r satisfies

$$d\tau = \sqrt{1 - \frac{r_s}{r}}\, dt, \tag{58}$$

where

$$r_s = \frac{2GM}{c^2}. \tag{59}$$

Define

$$\alpha(r) = \sqrt{1 - \frac{r_s}{r}}. \tag{60}$$

Then

$$d\tau = \alpha(r)dt. \tag{61}$$

Near the horizon, $\alpha(r) \to 0$. For an external observer using the asymptotic time coordinate t, internal processes appear slowed. For a local observer, local physics proceeds normally.

In this minimal approximation, one may write a readout-like shelter factor as

$$\mathcal{S} \sim \frac{1}{\alpha(r)}. \tag{62}$$

Thus, if $\alpha(r) \ll 1$, then $\mathcal{S} \gg 1$.

In the logarithmic rank notation introduced above, this same relation may be written as

$$r(r) = -\log_b \left(\sqrt{1 - \frac{2GM}{rc^2}} \right), \tag{63}$$

so that a large readout mismatch corresponds to a large rank difference:

$$\mathcal{S}_{A\to B} = \frac{\alpha_A}{\alpha_B} = b^{r_B - r_A}. \tag{64}$$

This shows how the operational frame notation connects back to standard relativistic lapse factors rather than replacing them by an unrelated rule.

This equation is not a complete cosmological model. It is only the minimal relativistic mechanism showing that external readout and local proper-time accumulation need not coincide. A developed model would have to specify the spacetime, congruence of observers, lapse function, matter content, and domain boundary conditions.

8. The Co-Falling Condition

A common objection is that if we were inside a strong gravitational or horizon-like domain, we should observe a large CMB dipole or strong anisotropy. This objection is serious, but it assumes that the observer moves through an external radiation bath.

The Temporal Shelter Hypothesis requires a different condition:

$$v_{\text{rel}} = v_{\text{observer}} - v_{\text{local field}} \approx 0. \tag{65}$$

That is, the observer, matter, radiation environment, and local measuring systems must be approximately co-falling or co-moving within the same domain.

In relativistic terms, the observed photon frequency is determined by

$$\nu_{\text{obs}} = -u^\mu k_\mu, \tag{66}$$

where u^μ is the observer four-velocity and k_μ is the photon wave-vector. A large anisotropic

Doppler signal requires a large relative velocity between the observer and the radiation frame. If the observer and local radiation environment share the same effective flow, the dominant dipole term is suppressed.

Therefore, the hypothesis does not predict a large CMB dipole merely from being in a gravitational domain. It predicts such a dipole only if the observer moves non-comovingly through the local radiation frame. This is a crucial restriction.

9. Isotropy Requirement

The CMB isotropy objection is among the strongest constraints. A viable temporal shelter model must satisfy

$$\left|\frac{\Delta T}{T}\right| \lesssim 10^{-5} \tag{67}$$

after subtracting the observed local dipole and known foregrounds, consistent with the observed smallness of CMB anisotropies [10, 9].

This means that the shelter domain, if relevant cosmologically, must be:

1. larger than the observable region or effectively homogeneous across it;
2. smooth enough that local tidal and lapse gradients are small;
3. co-falling with the radiation frame;
4. nearly isotropic around the observer over cosmological scales.

Thus the hypothesis does not work for a small, localized black-hole environment. If applied cosmologically, it only makes sense as a super-horizon-scale smooth gravitational domain or an equivalent phase-density background. This is not optional; it is required for consistency.

10. The Copernican Objection

Another objection is that placing life in a special near-horizon condition violates the Copernican principle. The response is not that Earth is central. The response is selection-based.

Life can only observe from regions where life can exist. If long biological time requires temporal shelter, observers will necessarily find themselves inside domains satisfying the shelter/readout condition. This is an anthropic selection effect, not a claim of spatial centrality.

The hypothesis replaces

$$\text{we are at a privileged spatial center} \tag{68}$$

with

$$\text{observers arise only in temporally protected domains.} \tag{69}$$

The selection condition is

$$T_{\text{local}} \geq T_{\text{bio}}. \tag{70}$$

Regions failing this condition do not produce observers capable of asking the question.

11. Fine-Tuning and the Size of the Gravitational Domain

The fine-tuning objection is also serious. Ordinary near-horizon environments can be destructive. A viable temporal shelter must satisfy two simultaneous conditions:

$$\alpha \ll 1, \tag{71}$$

and

$$\mathcal{T}_{\text{tidal}} \ll \mathcal{T}_{\text{bind}}, \tag{72}$$

where $\mathcal{T}_{\text{tidal}}$ represents local tidal stress and $\mathcal{T}_{\text{bind}}$ represents the binding strength of biological or astrophysical structures.

For a black hole of mass M, tidal gradients scale roughly as

$$\mathcal{T}_{\text{tidal}} \sim \frac{GM}{r^3}. \tag{73}$$

Near the horizon, $r \sim r_s \sim M$ in geometric units, so

$$\mathcal{T}_{\text{tidal}} \sim \frac{1}{M^2}. \tag{74}$$

Thus very massive horizon-like domains can produce strong relative time-dilation effects while maintaining weak local tidal gradients.

This is why the hypothesis must not be framed around small black holes. It requires an ultra-large, smooth, low-gradient gravitational domain:

$$M \gg M_{\text{stellar}}. \tag{75}$$

12. Thermodynamic Requirements

Time alone is not enough. A temporal shelter must also contain:

1. stable matter;
2. free energy;
3. entropy gradients;
4. long-lived stars or equivalent energy sources;
5. mechanisms for chemical complexity.

Therefore, the full life condition is not simply $\alpha \ll 1$. It is closer to

$$\alpha \ll 1, \qquad \nabla S \neq 0, \qquad E_{\text{free}} > 0, \qquad \mathcal{T}_{\text{tidal}} < \mathcal{T}_{\text{bind}}. \tag{76}$$

The Temporal Shelter Hypothesis only addresses the temporal component. It must be embedded in a broader physical model of matter, energy flow, and local thermodynamic disequilibrium.

13. Relation to Horizons

A horizon should not automatically be interpreted as local annihilation. Externally, a horizon is a boundary of return and readability. Internally, local proper time may remain well defined, depending on the spacetime and trajectory.

Thus

$$\text{external unreadability} \neq \text{internal nonexistence}. \tag{77}$$

In operational terms, a horizon can be treated as a limit of external reconstruction. It is not necessarily the end of internal dynamics. This interpretation is compatible with the broader relativistic view that horizons are observer-dependent causal boundaries rather than ordinary material surfaces [3, 5, 6].

14. Relation to Zero Theory Language

The present paper draws conceptual motivation from Zero Theory [26], but does not require the reader to accept the full framework. Only a minimal operational vocabulary is used.

The shared idea is that local physical time is counted by stable internal cycles:

$$T_{\text{local}} \propto N_{\text{cycles}}. \tag{78}$$

The cycle count is treated as internally real for the local system. What may differ between observers is the reconstruction of that cycle count as time, mass, scale, or horizon-readability.

This gives the operational rule:

$$\Delta_{\text{obs}}(X) = \Pi_{A\to B}(X) - X_A, \tag{79}$$

where X_A is the local frame description and $\Pi_{A\to B}(X)$ is the description reconstructed in frame B.

In this limited use, Zero Theory is not introduced as a complete replacement for general relativity or cosmology. It functions only as a language for distinguishing internal physical persistence from external readout.

15. Observer-Dependent Mass and Horizon-Like Readout

The observer-relative interpretation of temporal shelter is continuous with the broader Zero Theory idea that measured mass is not an isolated absolute property. In this view, observed mass is a readout rate: the rate at which internal phase cycles are counted by a given observer. If the observer and the target share the same gravitational or phase-readout environment, the measured mass is close to the locally defined rest value. If the observer and the target belong to different readout conditions, the inferred mass can change.

The same principle is applied here to horizons. A horizon-like condition is not first defined as an absolute internal catastrophe. It is defined as a relation between an internal domain and an external readout frame:

$$\text{horizon-like behavior} = \text{suppressed external readability of an internally coherent process.} \tag{80}$$

Thus, a domain may appear black-hole-like to a sufficiently different external observer while remaining locally ordinary to observers embedded in the same domain. The theory therefore does not require an absolute claim that an observer is "inside a black hole." It requires only the weaker and more operational claim that black-hole-like behavior is an external readout relation.

This distinction is central. The expected observational criteria must follow the observer-relative model. They should not require large universal echoes, large scalar polarizations, or generic violations of general relativity. Those would belong to a stronger and different claim. The present hypothesis expects weak, structured residuals associated with frame mismatch, lapse/readout gradients, compactness, or environmental phase-density differences.

16. Relation to Cosmology

The hypothesis can be applied weakly or strongly.

16.1. Weak Form

Strong gravitational or phase-density environments may increase the likelihood of long-lived biological domains by protecting local time. This version does not claim that the universe as a whole is inside a horizon-like shelter.

16.2. Strong Form

Our observed cosmic history may itself be an internal proper-time history as horizon-like or partially unreadable relative to a sufficiently different external readout frame. This strong form is not claimed here as established.

If the strong form is developed, it must reproduce:

1. CMB isotropy;
2. the Hubble relation;
3. BAO scale;
4. nucleosynthesis constraints;
5. structure formation;

6. local atomic-clock stability.

Until then, the strong cosmological version remains a research program rather than a completed model.

17. Galactic Clock-Domain Variant

The galactic version should not be interpreted as a claim that the Milky Way produces a strong Schwarzschild-like shelter factor. Classical gravitational time dilation across an ordinary galaxy is far too weak to yield $\mathcal{S} \gg 1$ by itself. Therefore, the galactic variant is not a strong temporal-shelter model in the same sense as a near-horizon lapse model.

Its more conservative role is different. A galaxy may be treated as a coherent operational clock-domain: a large system in which stars, gas, radiation, baryonic structure, dark matter phenomenology, and local observers share an approximately common dynamical and readout environment.

Thus the galactic domain is written as

$$\mathcal{D}_{\text{gal}} = \{\text{central compact object, stellar distribution, gas, halo, radiation frame, large-scale potential}\}. \tag{81}$$

The relevant condition is not

$$\mathcal{S}_{\text{gal}} \gg 1 \tag{82}$$

from classical galactic gravity. The conservative condition is instead

$$v_{\text{rel}} \approx 0, \qquad \nabla\alpha_{\text{gal}} \text{ small across the local biological domain,} \tag{83}$$

together with long-term dynamical stability:

$$T_{\text{local}} \geq T_{\text{bio}}. \tag{84}$$

The galactic variant is therefore useful for discussing co-falling clock coherence, not for claiming that galaxies are strong gravitational time shelters. Any stronger version would require an additional physical mechanism beyond the weak classical potential of an observed galaxy.

18. Observer-Dependent Horizons and Readout Boundaries

A central conceptual point is that a horizon is not an ordinary material wall. In general relativity, the event horizon is a causal boundary defined relative to the global structure of spacetime. For an external observer, infalling processes become increasingly redshifted and operationally unreconstructable. For a freely falling local observer crossing a sufficiently large smooth horizon, no local singular event need occur at the horizon itself [4, 5, 6].

The Temporal Shelter Hypothesis uses this distinction operationally. It does not require a horizon to be a place where internal physics stops. It requires only that external readout becomes incomplete or strongly distorted. Thus the key relation is

$$\text{horizon-like boundary} = \text{limit of external reconstruction}, \tag{85}$$

not

$$\text{horizon-like boundary} = \text{local destruction surface}. \tag{86}$$

This is why the hypothesis should not be phrased as a simple claim that life sits "inside a black hole." That phrasing invites the wrong objection. The more precise claim is that biological time may be protected inside a co-falling domain whose external readability is suppressed relative to its internal proper-time accumulation.

19. Existing Observational Motivations

The following observations are not presented as proof of the hypothesis. They are presented as classes of empirical tension that a temporal-shelter model would naturally ask us to re-examine. The distinction is essential: a scientific hypothesis should not merely attach itself to anomalies after the fact. It should turn them into quantitative diagnostics.

Until an explicit quantitative model is specified, these observations are not confirmations of the present framework. They are only candidate domains in which a readout-residual model could be tested and potentially falsified.

19.1. Early Supermassive Black Holes

One of the strongest observational motivations comes from massive black holes and active galactic nuclei at high redshift. JWST has intensified the question of how massive black holes and compact luminous systems appeared so early in cosmic history [23, 24]. In standard modeling, possible explanations include massive initial seeds, direct collapse channels, efficient gas inflow, and episodes of super-Eddington accretion.

In the shelter language, the relevant question is different: are some early-growth tensions partly symptoms of assigning a single global clock to systems whose internal structure may have accumulated time differently from an external cosmological readout? The hypothesis does not remove the need for astrophysical growth mechanisms. It asks whether the time available to those mechanisms should always be identified with one global FLRW clock.

A developed model would have to predict a measurable relation between black-hole mass, host-galaxy maturity, redshift, and local gravitational environment. Without such a relation, the idea remains explanatory rather than predictive.

19.2. CMB Low-Multipole Anomalies

The CMB is extremely isotropic, and that fact strongly constrains any shelter model. However, the largest angular scales have long displayed reported anomalies such as low quadrupole power, quadrupole-octupole alignment, hemispherical asymmetry, and the so-called axis-of-evil discussion [9, 10, 11]. These anomalies remain debated and may reflect cosmic variance, foregrounds, systematics, or statistical selection effects.

The shelter interpretation is not that these anomalies prove a boundary. A safer statement is that a co-falling domain with weak external-readout distortion might leave only low-multipole residuals rather than large local anisotropy. Therefore, the CMB test of the hypothesis is severe: any proposed shelter boundary must be compatible with the observed 10^{-5} anisotropy level while also predicting a specific residual pattern at low multipoles.

19.3. Gravitational-Wave Echoes and Near-Horizon Residuals

Late-time gravitational-wave echoes have been proposed as possible signatures of non-classical or nontrivial near-horizon structure. Claims of echoes remain controversial, and several analyses have found low statistical significance or sensitivity to methodology [19, 20, 25]. Therefore, echo-like features must not be treated as established evidence.

Nevertheless, they are relevant as a diagnostic class. If external reconstruction near a horizon-like boundary is incomplete, then delayed, suppressed, or phase-shifted signals are the natural type of observation to examine. The hypothesis should therefore predict not merely the existence of echoes, but their scaling with mass, spin, compactness, environmental potential, and propagation path.

19.4. Hubble and Growth Tensions

The Hubble tension and related growth-amplitude tensions are often discussed as possible signs that the minimal ΛCDM model is incomplete [15, 16]. Proposed responses include early dark energy, evolving dark energy, extra relativistic species, modified gravity, local structure effects, and calibration revisions.

The shelter hypothesis suggests another diagnostic possibility: some fraction of the discrepancy might be expressible as a mismatch between local clock calibration and global cosmological readout. This is not a solution by itself. A successful model would have to reproduce the CMB acoustic scale, BAO, supernova distances, nucleosynthesis, local distance ladders, and gravitational-wave standard-siren constraints in one timing framework.

20. Auxiliary Conceptual Burden and Model Economy

This paper does not argue that the standard cosmological model is wrong because it uses auxiliary concepts. Successful theories often introduce new entities or mechanisms that later become empirically established. The relevant question is narrower: can a proposed framework reduce the number of independent assumptions required to organize several residual phenomena?

The Temporal Shelter Hypothesis would be valuable only if a small number of operational principles - local proper-time accumulation, co-falling domains, observer-dependent readout, and horizon-like reconstruction limits - produced quantitative predictions with fewer adjustable assumptions than competing explanations.

This gives a methodological criterion:

> A theory becomes stronger when its auxiliary assumptions decrease as its observational range increases.

At the present stage, this criterion is a goal, not an achieved result. The framework must still demonstrate that its readout variables reduce explanatory cost rather than adding another unconstrained layer.

21. Observational Constraints

Any viable version must satisfy the following minimum constraints:

$$\left|\frac{\Delta T}{T}\right|_{\mathrm{CMB}} \lesssim 10^{-5}, \tag{87}$$

$$\mathcal{T}_{\mathrm{tidal}} < \mathcal{T}_{\mathrm{bind}}, \tag{88}$$

$$v_{\mathrm{rel}} \approx 0 \tag{89}$$

for the local radiation frame,

$$E_{\mathrm{free}} > 0, \tag{90}$$

and

$$T_{\mathrm{local}} \geq T_{\mathrm{bio}}. \tag{91}$$

These are not predictions yet. They are minimum consistency constraints. A model that cannot satisfy them is excluded.

22. Possible Predictions

A developed shelter model may differ from standard cosmology only if it predicts residuals not already absorbed by ordinary parameter fitting or known systematics. The main candidate classes are:

1. residual large-scale anisotropies after known dipoles and foregrounds are removed;
2. correlations between redshift residuals and gravitational or phase-density environment;
3. small apparent clock-rate distortions in transient timing;
4. weak phase-delay signatures near ultra-massive compact structures;
5. structured observer-relative residuals in near-horizon timing data.

The hypothesis becomes scientific only when at least one of these is made quantitative.

23. Composite Test Domains and Quantitative Anchors

The preceding sections produced two internal structural quantities:

$$r_{\mathrm{phys}} \approx 76.99, \qquad \Gamma_{\mathrm{ladder}} \approx 6.26.$$

These numbers were not fitted to astronomical data. The first follows from the laboratory-scale Compton/Planck ratio, and the second follows from applying the Race Protocol to the base-invariant ladder boundary $X \to 2X$. This section asks a different question: are there independent observational domains in which weak, structured, logarithmic or environment-correlated residuals have already been reported?

The answer is cautious. The reported data do not prove the framework. They do, however, provide quantitative anchors for future tests. The purpose of this section is therefore not to claim observational confirmation, but to show that the candidate test domains and numerical values are not introduced ad hoc.

23.1. Candidate A: Environmental Dependence of Type Ia Supernova Light Curves

Hypothesis. If effective clock readout correlates weakly with gravitational or phase-density environment, then astrophysical transients embedded in different host environments may show systematic timing or stretch residuals after standard corrections.

Current quantitative anchor. Type Ia supernova light-curve stretch x_1 is known to correlate with host-galaxy properties. A recent ZTF SN Ia DR2 analysis of a volume-limited sample of about 1,000 SNe Ia reports that the mean stretch distribution decreases with host stellar mass at 9.2σ significance [33]. The same study reports a nonlinear stretch-magnitude relation at 13.4σ, with a broken-α model:

$$x_1 < -0.48 \pm 0.08,$$

$$\alpha_{\text{low}} = 0.27 \pm 0.01, \qquad \alpha_{\text{high}} = 0.08 \pm 0.01,$$

and

$$\Delta_\alpha = -0.19 \pm 0.01.$$

It also finds an environmental magnitude offset greater than 0.12 mag for several tracers and approximately

$$\gamma_{\text{env}} \sim 0.17 \pm 0.01 \text{ mag}$$

when accounting for stretch nonlinearity.

Standard interpretation. These correlations are normally attributed to progenitor age, metallicity, host stellar population, star-formation history, and other environmental effects. The present framework does not reject that interpretation.

Discriminating power. The shelter framework suggests that a residual component of the stretch-environment relation may encode a weak observer-relative clock-rate or readout contribution. This requires a dedicated analysis separating progenitor-population effects from gravitational-potential, host-mass, or environment-correlated timing residuals. If no residual gravitational/readout component remains after such separation, this candidate weakens. If a residual persists with a scale correlated to the operational ladder estimate, the framework gains empirical motivation.

23.2. Candidate B: Reported Log-Periodic Clustering in Redshifts

Hypothesis. A discrete or approximately discrete scale structure in operational readout could appear as a log-periodic modulation in the redshift distribution of distant sources.

Current quantitative anchor. Karlsson-type periodicity has been discussed since the 1970s [27, 28]. A recent re-analysis by Mal et al. [29] reports fundamental periodicities

$$\Delta \log_{10}(1+z) \approx 0.077, \qquad \Delta \log_{10}(1+z) \approx 0.089$$

in 2dF and SDSS quasar-galaxy pair datasets at a reported 95% confidence level. The same work reports a linear-scale periodicity near 0.051 in SDSS DR7.

The value most relevant to the historical Karlsson sequence is

$$\Delta_{\mathrm{K}} \equiv \Delta \log_{10}(1+z) \approx 0.089.$$

The binary structural rung in base-10 logarithmic units is

$$\Delta_2 = \log_{10} 2 \approx 0.3010.$$

Thus, if the Karlsson-type spacing is physically meaningful, it is not a replacement for the binary rung. It is closer to a fractional or sub-rung scale:

$$\frac{\Delta_{\mathrm{K}}}{\Delta_2} = \frac{0.089}{0.3010} \approx 0.296.$$

Equivalently, the binary rung contains about

$$\frac{\Delta_2}{\Delta_{\mathrm{K}}} \approx 3.38$$

such reported Karlsson intervals.

Standard interpretation. Redshift quantization is not part of standard cosmology. The mainstream interpretation treats such signals as selection effects, aliasing, survey-window artifacts, source clustering, or statistical fluctuations rather than intrinsic redshift quantization.

Discriminating power. The present framework does not require redshift periodicity to be real. If future high-precision surveys rule it out, the empirical cross-calibration branch is weakened or removed. If a stable log-periodic spacing survives independent surveys and selection-function tests, the framework provides a possible operational context: such a spacing could be interpreted as a fractional rung or observational projection of an underlying logarithmic ladder.

23.3. Candidate C: Log-Periodic Oscillations in CMB and Gravitational-Wave Backgrounds

Hypothesis. If discrete scale invariance is part of the effective readout structure, it may leave log-periodic modulations in cosmological observables such as the primordial power spectrum or stochastic gravitational-wave background.

Current quantitative anchor. Discrete scale invariance is a recognized theoretical mechanism for log-periodic structures [30]. In multi-scale and quantum-gravity-inspired frameworks, log-periodic modulations can appear in cosmological observables [31]. Calcagni and Kuroyanagi [32] specifically show that log-periodic structures can generate a stochastic gravitational-wave background beyond Einstein gravity.

On the CMB side, a recent analysis using ACT DR6, SPT-3G, and Planck data reports a tightened upper bound on logarithmic and linear primordial oscillations:

$$A_{\mathrm{log,lin}} \lesssim 0.029 \qquad (95\% \text{ C.L.}),$$

with no hint for primordial oscillations [34]. No dedicated published test has yet targeted the particular period $\log_{10} 2 \approx 0.301$ or its fractional projections in the present operational-ladder sense.

Standard interpretation. Minimal ΛCDM does not predict a log-periodic primordial modulation. Searches for such oscillations are usually treated as constraints on inflationary features or physics beyond the simplest slow-roll models.

Discriminating power. The current CMB bound is a constraint, not confirmation. The toy model in this paper uses residual amplitudes of order 10^{-6}, far below $A_{\mathrm{log,lin}} \sim 0.029$. Future CMB-S4, LISA, Einstein Telescope, Cosmic Explorer, and pulsar-timing analyses may provide more direct constraints on log-periodic or discrete-scale-invariant readout structures.

23.4. Composite Signature Logic

The three domains above are deliberately heterogeneous. Each has a standard interpretation:

1. SN Ia stretch-environment dependence is usually attributed to progenitor/environment physics.
2. Karlsson-type redshift periodicity is usually treated as controversial and possibly systematic.
3. Log-periodic CMB/GW oscillations are usually treated as constraints on primordial features or beyond-ΛCDM physics.

The shelter framework does not become credible by attaching itself to any one of these. It becomes scientifically interesting only if future analyses reveal a shared pattern: weak, structured residuals correlated with operational frame mismatch, environmental depth, or logarithmic scale structure.

Domain	Quantitative anchor	Standard view	Role in this framework
SN Ia stretch vs. environment	9.2σ stretch-host mass dependence; $\gamma_{\rm env} \sim 0.17 \pm 0.01$ mag	Progenitor/environment effect	Search for residual clock/readout component
Redshift periodicity	Reported $0.077, 0.089$ log spacings at 95% confidence	Selection or survey artifact	Possible fractional rung if independently confirmed
CMB/GW log-periodicity	$A_{\rm log,lin} \lesssim 0.029$ at 95% C.L.; no current hint	Constraint on primordial features	Future bound on DSI/readout modulation

The framework does not require any single candidate to be confirmed. Its scientific value would increase only if independent residuals converge toward the same calibrated operational scale. Conversely, if dedicated searches find no residual environmental clock component in SNe Ia, no robust log-periodic structure in redshifts, and increasingly strong upper limits on log-periodic CMB/GW modulations, then the hypothesis loses empirical support.

The important point is methodological: the numerical values in this section are not chosen freely. They are imported from reported observational analyses and used as test anchors. The framework remains conservative by treating them as constraints and search targets rather than as proof.

24. Mock-Data Sensitivity Test for the Structural Frequency

Section 23 identified observational domains in which structured residuals may be searched for. This section adds a deliberately limited numerical test. It does not analyze DESI, Euclid, or any real galaxy-correlation catalogue. Its purpose is narrower: to verify that a weak log-periodic residual at the structurally predicted frequency can be recovered from noisy correlation-function-like mock data using a blind frequency scan.

24.1. Predicted Search Frequency

The binary operational rung corresponds to

$$\Delta_2 = \log_{10} 2 \simeq 0.3010. \tag{92}$$

The corresponding frequency in $\log_{10} s$, where s is a comoving separation, is

$$f_{\rm struct} = \frac{1}{\log_{10} 2} = 3.321928\ldots. \tag{93}$$

A phenomenological residual in the two-point correlation function may therefore be written as

$$\delta_\xi^{\rm LP}(s) = A_\xi \cos(2\pi f_{\rm struct} \log_{10} s + \phi)\,, \tag{94}$$

where A_ξ is a small residual amplitude and ϕ is an unknown phase.

24.2. Mock Construction

A smooth fiducial correlation-like curve was generated over

$$5 \le s \le 300\ h^{-1}\mathrm{Mpc}$$

with a broad BAO-like bump. A weak log-periodic component at $f_{\rm struct}$ was injected into the residual, together with Gaussian noise and low-frequency nuisance trends representing imperfect fiducial subtraction or survey-window residuals. A blind sinusoidal frequency scan was then performed over

$$0.4 \le f \le 8.0.$$

For each injected amplitude, 500 Monte Carlo realizations were generated.

The null case $A_\xi = 0$ was used to define empirical max-power thresholds. In this mock setup the null thresholds were

$$P_{95} = 0.0666, \qquad P_{99} = 0.0850.$$

24.3. Monte Carlo Recovery Results

The recovery criterion was that the best-fit frequency lie within

$$|f_{\rm rec} - f_{\rm struct}| \le 0.08$$

of the structural frequency. The results are summarized in Table 1.

A_ξ	**Near-target rate**	**Near target + 95% null**	**Near target + 99% null**	**Median recovered amplitude**
0.000	0.006	0.000	0.000	0.0034
0.004	0.580	0.258	0.108	0.0044
0.006	0.888	0.862	0.750	0.0061
0.008	0.970	0.970	0.970	0.0082
0.010	0.998	0.998	0.998	0.0101
0.012	0.998	0.998	0.998	0.0120
0.016	1.000	1.000	1.000	0.0160
0.020	1.000	1.000	1.000	0.0200

Table 1: Monte Carlo recovery of the structural log-periodic frequency in noisy mock residuals.

The null case produced a false near-target recovery rate of only 0.6%. For injected amplitudes $A_\xi \gtrsim 0.006$, the structural frequency was recovered in more than 88% of realizations. For $A_\xi \gtrsim 0.008$, recovery above the 99% null threshold approached unity in this simplified setup.

24.4. Figures

Figure 1 shows the recovery rate as a function of injected amplitude. Figure 2 shows the distribution of recovered best frequencies for selected injected amplitudes. Figure 3 shows a representative blind frequency scan for $A_\xi = 0.010$.

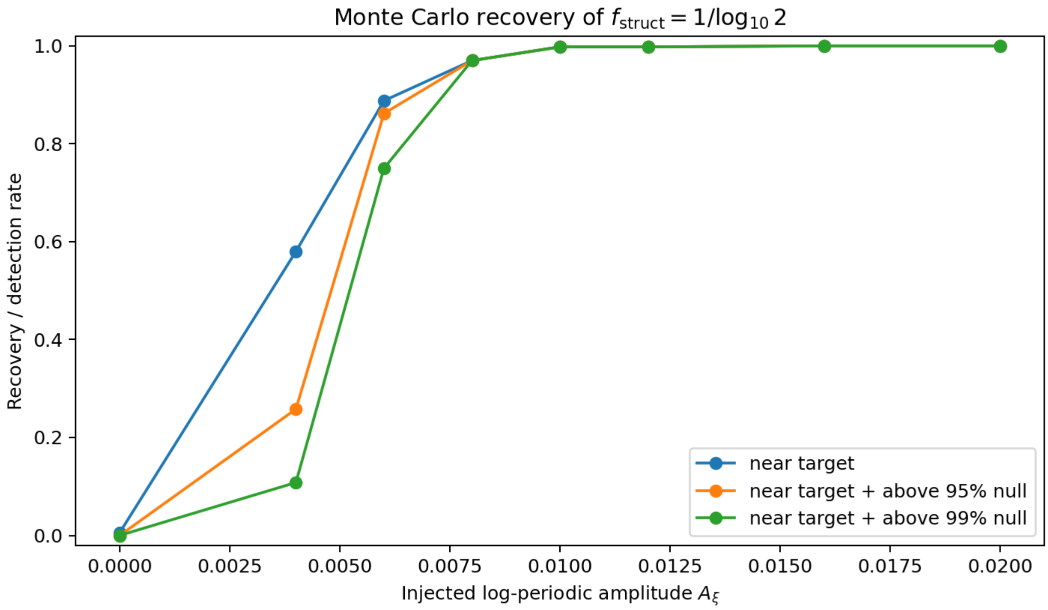

Figure 1: Monte Carlo recovery rate for the structurally predicted frequency $f_{\mathrm{struct}} = 1/\log_{10} 2$.

24.5. Interpretation and Limitation

This test does not prove that large-scale structure contains the predicted modulation. It shows only that the proposed frequency is operationally searchable: if a residual of this form exists at the tested amplitude scale, a direct frequency-domain method can recover it from noisy mock residuals. A real survey analysis would require covariance matrices, survey-window functions, redshift-space distortions, BAO marginalization, mock catalogues, and look-elsewhere corrections.

The result nevertheless strengthens the programmatic claim of the paper. The framework no longer merely identifies qualitative observational domains; it supplies a non-arbitrary search frequency and demonstrates that this frequency can be recovered in controlled mock data.

25. A Minimal Quantitative Toy Model

To avoid leaving the framework entirely qualitative, this section introduces a deliberately simple toy model. It is not intended as a full cosmological solution. Its purpose is to

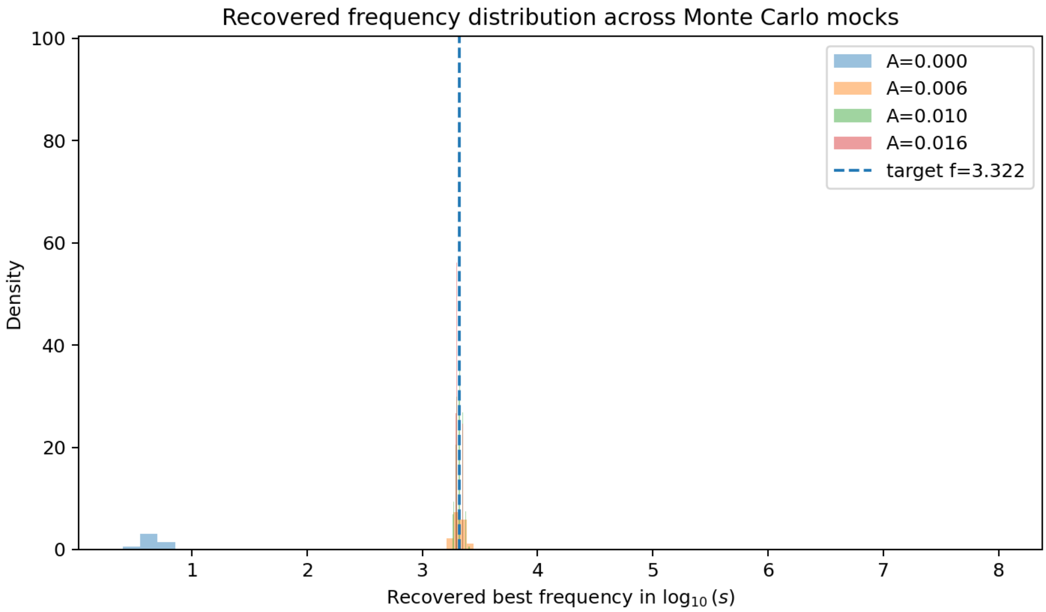

Figure 2: Recovered best-frequency distributions across Monte Carlo mock realizations.

show how a weak observer-relative readout residual can be parameterized, constrained, and compared with data.

Consider a smooth effective readout perturbation relative to a background frame:

$$\alpha_{\text{eff}}(\chi, \hat{\mathbf{n}}) = 1 - \epsilon\, F(\chi, \hat{\mathbf{n}}), \tag{95}$$

where $0 < \epsilon \ll 1$, χ is a radial or lookback coordinate, $\hat{\mathbf{n}}$ is direction on the sky, and F is a dimensionless profile normalized so that

$$|F| \leq 1. \tag{96}$$

For weak perturbations,

$$r_{\text{eff}} = -\log_b(\alpha_{\text{eff}}) \simeq \frac{\epsilon F}{\ln b}. \tag{97}$$

For the binary choice $b = 2$,

$$r_{\text{eff}} \simeq \frac{\epsilon F}{\ln 2}. \tag{98}$$

The corresponding readout factor between an unperturbed frame and the perturbed frame is, to first order,

$$\mathcal{S}_{\text{eff}} = \frac{1}{\alpha_{\text{eff}}} \simeq 1 + \epsilon F. \tag{99}$$

If such a perturbation contributes to a temperature or redshift readout, the leading residual has the order

$$\left|\frac{\delta T}{T}\right| \sim \left|\frac{\delta z}{1+z}\right| \sim \epsilon |F|. \tag{100}$$

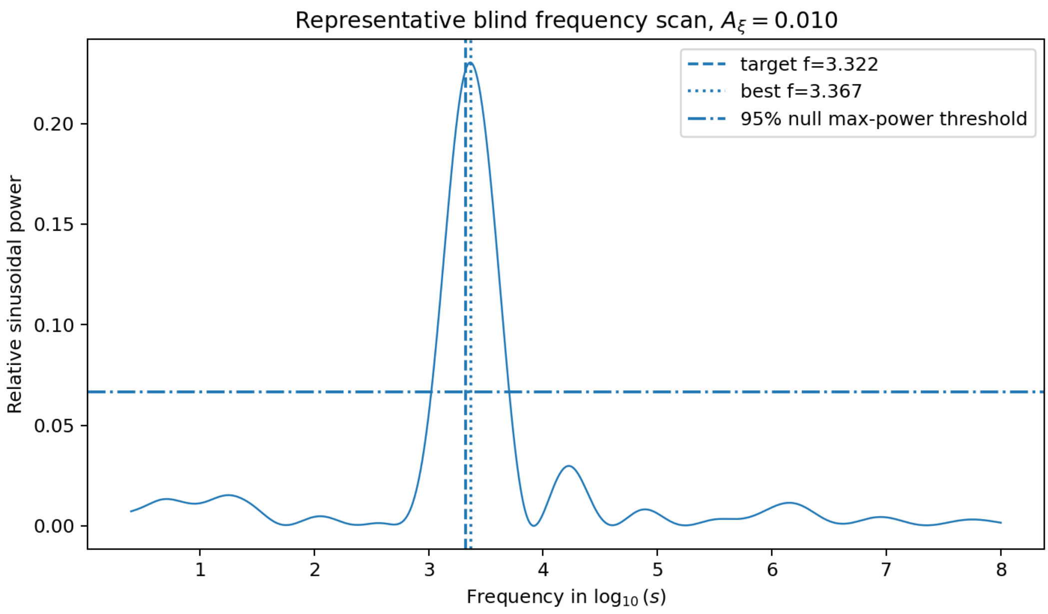

Figure 3: Representative blind frequency scan for an injected amplitude $A_\xi = 0.010$.

The observed CMB anisotropy level imposes the rough consistency requirement

$$\epsilon \lesssim 10^{-5} \tag{101}$$

for a cosmological-scale residual that projects onto the CMB without being absorbed into the monopole or dipole.

As a concrete numerical illustration, choose

$$\epsilon = 10^{-6}. \tag{102}$$

Then the maximum binary rank perturbation is

$$|r_{\text{eff}}|_{\max} \simeq \frac{10^{-6}}{\ln 2} \simeq 1.44 \times 10^{-6}. \tag{103}$$

The corresponding maximum readout residual is

$$\left|\frac{\delta T}{T}\right|_{\max} \sim 10^{-6}, \tag{104}$$

which is below the primary 10^{-5} CMB anisotropy scale but potentially within the conceptual domain of low-multipole residual searches.

This toy model does not prove the Temporal Shelter Hypothesis. It demonstrates only that the operational-rank notation can be connected to a measurable residual scale. A strong temporal shelter with $\mathcal{S} \gg 1$ would require much smaller α_{eff} and would therefore be severely constrained by CMB isotropy unless the domain is extremely smooth, co-falling, or externally projected mainly into unobservable monopole-like components.

26. Toward Quantitative Predictions

The present paper deliberately does not assign premature numerical values to the shelter factor, the effective lapse, or the amplitude of possible near-horizon residuals. Such numbers would be misleading unless a specific domain geometry, lapse profile, observer congruence, matter distribution, and boundary condition were first defined.

Nevertheless, the hypothesis can be made progressively quantitative. The next stage of the program is to extract a small set of measurable quantities from an explicit model. The minimal quantities are:

$$\alpha_{\rm eff}(x^\mu), \tag{105}$$

$$r_{\rm eff}(x^\mu) = -\log_b \alpha_{\rm eff}(x^\mu), \tag{106}$$

$$\mathcal{S}_{A\to B} = \frac{\alpha_A}{\alpha_B} = b^{r_B - r_A}, \tag{107}$$

and

$$R_b = \frac{A_b}{A_T}. \tag{108}$$

Here $\alpha_{\rm eff}$ denotes an effective lapse or external-readout factor, $\mathcal{S}_{A\to B}$ denotes the corresponding inter-frame shelter/readout factor, and R_b denotes a phenomenological ratio of a possible scalar, breathing-like, or readout-residual amplitude to the ordinary tensor amplitude in a gravitational-wave signal. In this paper R_b is not derived from a completed modified-gravity field equation; it is included only as a placeholder for a future waveform-level parameterization.

The hypothesis therefore makes no claim of the form

$$R_b = 0.003 \tag{109}$$

at the present stage. A fixed number of this kind would require a completed dynamical model. Instead, the current paper makes the weaker but testable programmatic claim that any viable quantitative version must eventually produce functions of the form

$$\alpha_{\rm eff} = \alpha_{\rm eff}(M, \chi, r, t, \rho_{\rm env}, \mathcal{D}), \tag{110}$$

$$\mathcal{S}_{\rm eff} = \mathcal{S}_{\rm eff}(M, \chi, r, t, \rho_{\rm env}, \mathcal{D}), \tag{111}$$

and

$$R_b = R_b(M, \chi, f, \mathcal{C}, \rho_{\rm env}), \tag{112}$$

where M is the characteristic mass scale, χ is a spin parameter, r is a radial or domain coordinate, f is the gravitational-wave frequency, $\mathcal{C}$ is compactness, $\rho_{\rm env}$ denotes environmental density or phase-density structure, and $\mathcal{D}$ denotes the relevant co-falling domain.

This gives a concrete path from hypothesis to model:

1. define an explicit lapse or readout profile α_{eff} for a candidate shelter domain;
2. compute the shelter factor $\mathcal{S}_{\text{eff}}$ and check whether it can support long internal proper time without violating CMB and tidal constraints;
3. derive predicted residuals in black-hole ringdown, electromagnetic timing, or redshift-environment correlations;
4. compare those residuals with LIGO/Virgo/KAGRA, pulsar-timing arrays, Event Horizon Telescope timing, supernova residuals, and CMB low-multipole data.

26.1. Minimal Effective Readout Profile for the Next Stage

The next natural step is the construction of a minimal effective readout profile. The present paper does not introduce this profile as a derived field equation. It is included only to specify the immediate continuation of the program and to prevent the symbol α_{eff} from remaining purely formal.

A minimal phenomenological profile can be written as

$$\alpha_{\text{eff}}(x^\mu) = R_{\text{ladder}}\,\alpha_{\text{geom}}(x^\mu)\left[1 + A\cos(2\pi f_{\text{struct}}\log_{10} Q(x^\mu) + \phi) + \eta E(x^\mu)\right], \tag{113}$$

where

$$R_{\text{ladder}} = 0.159624\ldots, \qquad f_{\text{struct}} = \frac{1}{\log_{10} 2} = 3.321928\ldots.$$

Here $\alpha_{\text{geom}}(x^\mu)$ denotes the ordinary geometric or lapse-like contribution; $Q(x^\mu)$ denotes the observational scale relevant to the chosen test domain; $E(x^\mu)$ denotes an environmental variable such as host potential, compactness, density, or phase-density proxy; and A, ϕ, η are phenomenological parameters.

For the large-scale-structure branch tested in the mock-data section, the simplest specialization is

$$Q(x^\mu) \to s, \tag{114}$$

so that

$$\alpha_{\text{eff}}^{\text{LSS}}(s) = \alpha_0\left[1 + A_\xi\cos(2\pi f_{\text{struct}}\log_{10} s + \phi)\right]. \tag{115}$$

After the smooth monopole-like factor α_0 is absorbed into the background calibration, the observable residual takes the form already used in the mock sensitivity test:

$$\delta_\xi(s) \sim A_\xi\cos(2\pi f_{\text{struct}}\log_{10} s + \phi). \tag{116}$$

Equation (113) is therefore not a completed theory of α_{eff}. It is a disciplined bridge between the present programmatic framework and the next phenomenological model. A derived dynamical profile would require a specific metric, field equation, matter distribution, boundary condition, and observer congruence.

Thus the present paper should be read as a constrained hypothesis and not as a completed numerical theory. Its falsifiability improves as soon as a specific α_{eff} profile is chosen. Once that profile is specified, non-observation of the predicted residuals within the relevant sensitivity range would count against the corresponding model version.

27. Status of Claims and Failure Modes

To prevent the hypothesis from being interpreted as a completed cosmological model, the main claims can be classified as follows:

Statement	Status	Required Test
Long biological time requires local temporal stability	Conceptual premise	Compare biological and evolutionary timescales with local clock stability conditions
Gravitational time dilation can provide external slowing	Derived from relativity	Requires explicit metric and congruence specification
Temporal shelter domains may support long internal histories	Hypothesis	Must satisfy CMB, tidal, thermodynamic, and clock constraints
Galaxies may act as coherent clock-domains	Weak model variant	Requires dynamical coherence, not strong lapse amplification
Observed domains may appear horizon-like to sufficiently different external readout frames	Strong observer-relative form	Must reproduce CMB, BAO, nucleosynthesis, structure formation, and local clocks

The most dangerous failure modes of the hypothesis are:

1. production of CMB anisotropy larger than observed limits;
2. destructive tidal gradients in the proposed shelter domain;
3. absence of free energy or thermodynamic gradients;
4. failure to reproduce BAO, nucleosynthesis, and structure formation;
5. lack of any quantitative prediction distinguishable from standard cosmology;
6. inability to identify a measurable residual associated with lapse/readout structure.

Thus, the hypothesis is not protected from falsification. It becomes weaker if it remains only interpretive, and stronger only if it predicts a measurable residual.

28. Why This Is Not a Black-Hole Habitability Claim

The Temporal Shelter Hypothesis should not be confused with the claim that ordinary black holes are habitable. A stellar-mass or small black hole generally provides neither a stable biological environment nor tolerable tidal conditions. The relevant object, if the hypothesis is physically meaningful, must be an ultra-large, smooth, low-gradient gravitational or phase-density domain.

Therefore, the phrase "near-horizon" should be understood operationally:

$$\text{near-horizon} \neq \text{near a destructive small black hole.} \tag{117}$$

Rather, it means:

$$\text{near-horizon} = \text{a regime where external readout is strongly suppressed while local dynamics remain co} \tag{118}$$

This distinction is essential. The hypothesis concerns protected proper time, not biological life on or near an ordinary event horizon.

29. Observer-Relative Observational Criteria

The hypothesis should not force an observational package that contradicts its own core principle. In this framework, black-hole-like behavior is not treated as an absolute statement about location. It is treated as an observer-dependent readout relation:

$$\text{black-hole-like} \equiv \text{external unreadability relative to a sufficiently different observer.} \tag{119}$$

Therefore the relevant observations should not be framed as evidence that "we are inside a black hole." They should be framed as evidence for a mismatch between local normality and external geometric readability.

A single anomaly would not be decisive. The most meaningful support would be a coherent package of weak, structured, observer-relative residuals that are difficult to reduce to isolated noise, foregrounds, or ordinary modeling error. Such a package should satisfy the following conditions:

1. local physical normality is preserved: local clocks, spectra, chemistry, orbital dynamics, and causal continuity remain internally coherent;

2. external readout is systematically distorted: the same domain appears slowed, compressed, over-massive, redshifted, or partially unreadable to an external or differently situated observer;

3. the distortion correlates with gravitational potential, compactness, phase-density environment, or observer-frame mismatch rather than appearing as arbitrary noise;

4. the effect is weak and residual-like in ordinary observational regimes, not a large universal violation of general relativity;

5. any gravitational-wave component beyond the tensor channel is small, conditional, and regime-dependent rather than large and generic;

6. the pattern recurs across independent systems after known systematics and foregrounds are removed.

This observer-relative package is more faithful to the hypothesis than a demand for a large echo, a large scalar mode, or an obvious breakdown of Kerr geometry in every black-hole merger. The expected signal is not a dramatic failure of standard physics, but a systematic residue at the boundary between local physical coherence and external readability.

In gravitational-wave language, the near-horizon version of this criterion may be written schematically as

$$\text{Kerr-consistent leading signal} + \text{weak structured residual} + \text{observer/readout phase delay} + R_b \ll 1, \tag{120}$$

where

$$R_b = \frac{A_b}{A_T} \tag{121}$$

denotes the phenomenological ratio of a possible scalar, breathing-like, or readout-residual amplitude to the ordinary tensor amplitude. A future dynamical model would need to specify the waveform decomposition in which A_b and A_T are measured.

The important point is not that R_b must be large. On the contrary, the observer-dependent model expects any non-tensorial or readout-like contribution to be weak, conditional, and visible only in special regimes. A large universal scalar mode would belong to a different and more extreme theory, not to the present one.

Thus the strongest observational support would not be one spectacular anomaly. It would be a repeated correlation:

$$\text{local normality} + \text{external readout distortion} + \text{environment/compactness scaling} + \text{weak structured residu} \tag{122}$$

This is the intended observational criterion of the present paper.

30. Relation to Projectability-Based Approaches

This hypothesis is compatible with, but does not depend on, approaches in which spacetime geometry is treated as an effective projection rather than a primitive substrate. In such approaches, horizons may be interpreted as boundaries where geometric projectability weakens or fails.

The Temporal Shelter Hypothesis adds a biological and observer-operational interpretation to this idea:

$$\text{failure of external projectability} \quad \not\Rightarrow \quad \text{failure of internal history}. \tag{123}$$

Instead,

$$\text{external unreadability} \quad \text{may coexist with} \quad \text{long internal proper time.} \tag{124}$$

This is the central conceptual bridge between horizon physics and biological time.

31. Conservative Final Statement

The strongest version would claim:

> Civilization requires near-horizon time dilation.

That is not established.

The conservative version defended here is:

> Long biological evolution may require protected local time, and gravitational or phase-density time dilation is a possible physical mechanism for such protection.

This is not yet a complete theory. It is a structured hypothesis.

32. Conclusion

The revised Temporal Shelter Hypothesis does not claim that civilization literally inhabits an ordinary astrophysical black hole. Its claim is operational and observer-relative: long biological history depends on locally coherent proper-time accumulation, while the external reconstruction of that history may vary across operational frames.

The present paper advances this framework in four concrete steps.

1. The Planck scale is treated as an operational baseline, and the electron Compton wavelength is used to calibrate the present frame, yielding

   $$r_{\text{phys}} \approx 76.99$$

   in the binary ladder.

2. The Phase-Capacity Race Protocol converts a progress share k into an internal recurrence factor $R = \sqrt{1-k^2}$ and a slowdown factor $\Gamma = 1/R$.

3. The progress share is written in a base-invariant form,

   $$k = \frac{\log_b X}{\log_b(2X)}, \qquad X = \frac{\lambda_C}{l_P},$$

   so that the result does not depend on the logarithmic coordinate used to describe the ladder.

4. The resulting ladder estimate,
$$\Gamma_{\rm ladder} \approx 6.26,$$
is classified as a heuristic compression-depth estimator, not as a direct empirical measurement of time dilation.

The hypothesis shifts attention away from the absolute statement

"we are inside a black hole"

and toward the weaker and more physical statement

black-hole-like behavior = observer-dependent external unreadability.

The scientific value of the proposal depends on whether operational frame mismatch leaves measurable residuals. The candidate observational domains discussed here - environmental dependencies of Type Ia supernova light curves, reported log-periodic redshift structure, and CMB/GW log-periodic constraints - are not treated as evidence. They are treated as quantitative test domains whose numerical anchors come from reported observational analyses. The mock-data recovery test shows that the non-arbitrary structural frequency $f_{mstruct} = 1/\log_{10} 2$ can be recovered from noisy synthetic residuals at the tested amplitude scale.

The present manuscript should therefore be interpreted as a constrained research program. Its next stage is the derivation of explicit lapse/readout profiles and the quantitative comparison of predicted observer-relative residuals with supernova, CMB, gravitational-wave, and horizon-scale timing data.

Acknowledgment

This manuscript was prepared as part of an independent conceptual research program on black-hole and cosmological time concepts.

Project Identity

This manuscript is released under the project identity "Independent Research Collaboration on Black Hole and Cosmology Concepts" (IRCBHC). IRCBHC is used here as a project designation for an independent research program.

ORCID record associated with the framework: [insert ORCID].

References

[1] E. Tiesinga, P. J. Mohr, D. B. Newell, and B. N. Taylor, "CODATA recommended values of the fundamental physical constants: 2022," National Institute of Standards and Technology, 2022.

[2] A. Einstein, "Die Grundlage der allgemeinen Relativitaetstheorie," *Annalen der Physik*, vol. 354, no. 7, pp. 769–822, 1916.

[3] S. W. Hawking and G. F. R. Ellis, *The Large Scale Structure of Space-Time*. Cambridge University Press, 1973.

[4] C. W. Misner, K. S. Thorne, and J. A. Wheeler, *Gravitation*. W. H. Freeman, 1973.

[5] R. M. Wald, *General Relativity*. University of Chicago Press, 1984.

[6] S. M. Carroll, *Spacetime and Geometry: An Introduction to General Relativity*. Addison-Wesley, 2004.

[7] S. Weinberg, *Cosmology*. Oxford University Press, 2008.

[8] S. Dodelson, *Modern Cosmology*. Academic Press, 2003.

[9] C. L. Bennett et al., "Nine-year Wilkinson Microwave Anisotropy Probe (WMAP) observations: final maps and results," *Astrophysical Journal Supplement Series*, vol. 208, 20, 2013.

[10] N. Aghanim et al. (Planck Collaboration), "Planck 2018 results. VI. Cosmological parameters," *Astronomy & Astrophysics*, vol. 641, A6, 2020.

[11] D. J. Schwarz, C. J. Copi, D. Huterer, and G. D. Starkman, "CMB anomalies after Planck," *Classical and Quantum Gravity*, vol. 33, 184001, 2016.

[12] A. G. Riess et al., "Observational evidence from supernovae for an accelerating universe and a cosmological constant," *Astronomical Journal*, vol. 116, pp. 1009–1038, 1998.

[13] S. Perlmutter et al., "Measurements of Omega and Lambda from 42 high-redshift supernovae," *Astrophysical Journal*, vol. 517, pp. 565–586, 1999.

[14] D. J. Eisenstein et al., "Detection of the baryon acoustic peak in the large-scale correlation function of SDSS luminous red galaxies," *Astrophysical Journal*, vol. 633, pp. 560–574, 2005.

[15] L. Verde, T. Treu, and A. G. Riess, "Tensions between the early and late Universe," *Nature Astronomy*, vol. 3, pp. 891–895, 2019.

[16] A. G. Riess et al., "A comprehensive measurement of the local value of the Hubble constant with 1 km s^{-1} Mpc^{-1} uncertainty from the Hubble Space Telescope and the SH0ES Team," *Astrophysical Journal Letters*, vol. 934, L7, 2022.

[17] B. P. Abbott et al. (LIGO Scientific Collaboration and Virgo Collaboration), "Observation of gravitational waves from a binary black hole merger," *Physical Review Letters*, vol. 116, 061102, 2016.

[18] B. P. Abbott et al. (LIGO Scientific Collaboration and Virgo Collaboration), "Tests of general relativity with GWTC-1," *Physical Review D*, vol. 100, 104036, 2019.

[19] V. Cardoso, V. F. Foit, and M. Kleban, "Gravitational wave echoes from black hole area quantization," *Journal of Cosmology and Astroparticle Physics*, 2019, 006, 2019.

[20] J. Westerweck et al., "Low significance of evidence for black hole echoes in gravitational wave data," *Physical Review D*, vol. 97, 124037, 2018.

[21] Event Horizon Telescope Collaboration, "First M87 Event Horizon Telescope results. I. The shadow of the supermassive black hole," *Astrophysical Journal Letters*, vol. 875, L1, 2019.

[22] Event Horizon Telescope Collaboration, "First Sagittarius A* Event Horizon Telescope results. I. The shadow of the supermassive black hole in the center of the Milky Way," *Astrophysical Journal Letters*, vol. 930, L12, 2022.

[23] I. Labbe et al., "A population of red candidate massive galaxies $\sim$600 Myr after the Big Bang," *Nature*, vol. 616, pp. 266–269, 2023.

[24] M. Boylan-Kolchin, "Stress testing ΛCDM with high-redshift galaxy candidates," *Nature Astronomy*, vol. 7, pp. 731–735, 2023.

[25] N. Uchikata, S. Yoshida, and T. P. Sotiriou, "Searching for gravitational wave echoes from black hole area quantization," *Physical Review D*, vol. 108, 104040, 2023.

[26] IRCBHC, *Zero Theory*, Zenodo, 2026. doi:10.5281/zenodo.20473408.

[27] K. G. Karlsson, "Possible discretization of quasar redshifts," *Astronomy & Astrophysics*, vol. 13, pp. 333–335, 1971.

[28] K. G. Karlsson, "Quasar redshifts and nearby galaxies," *Astronomy & Astrophysics*, vol. 239, pp. 50–56, 1990.

[29] A. Mal, S. Palit, C. C. Fulton, and S. Roy, "Quantized Redshift and its significance for recent observations," *Research in Astronomy and Astrophysics*, vol. 24, 095014, 2024. arXiv:2408.07101.

[30] D. Sornette, "Discrete scale invariance and complex dimensions," *Physics Reports*, vol. 297, pp. 239–270, 1998. arXiv:cond-mat/9707012.

[31] G. Calcagni, "Multi-scale gravity and cosmology," *Journal of Cosmology and Astroparticle Physics*, vol. 2013, no. 12, 041, 2013. arXiv:1307.6382.

[32] G. Calcagni and S. Kuroyanagi, "Log-periodic gravitational-wave background beyond Einstein gravity," *Classical and Quantum Gravity*, vol. 41, 015031, 2024. arXiv:2308.05904.

[33] M. Ginolin et al., "ZTF SN Ia DR2: Environmental dependencies of stretch and luminosity of a volume limited sample of 1,000 Type Ia Supernovae," *Astronomy & Astrophysics*, vol. 695, A140, 2025. arXiv:2405.20965.

[34] Z.-Y. Peng and Y.-S. Piao, "Tightening constraints on primordial oscillations with latest ACT and SPT data," arXiv:2507.17276, 2025.